BMC Veterinary Research

RESEARCH

Open Access

Identification of interferon-stimulated response elements (ISREs) in canines

Zhichao Pan[1†], Yutong Liu[1†], Huilin Dai[1], Siqi Xu[1], Miaomiao Qin[1], Ke Wang[1], Chenying Luo[1], Changqi Luo[1], Qinying Zhang[1], Zhaoping Liang[1,2,3,4,5*] and Saixiang Feng[1,2,3,4,5*]

Abstract

Interferon (IFN) responses are vital for antiviral defense, with interferon-stimulated response elements (ISREs) crucial for regulating IFN signaling. While ISREs are well-studied in humans and mice, research on canine ISREs is limited. This study aimed to clarify the role of canine ISREs and create a new method for detecting IFN activity. Canine IFN α (CaIFNα) was produced using the *Pichia pastoris* (*P. pastoris*) system, and an ISRE-based flow cytometry method was developed to measure its activity. ISREs for CaIFNα were predicted via bioinformatics analysis. Subsequently, viral suppression assays were conducted using vesicular stomatitis virus, canine influenza virus, and H9N2 to evaluate the antiviral activity of recombinant CaIFNα. Fluorescence analysis confirmed that CaIFNα activates ISRE2, ISRE8, and ISRE10, thereby enhancing the transcription and expression of the enhanced green fluorescent protein (EGFP) fusion gene. A novel ISRE and EGFP based flow cytometry method enabled precise quantification of CaIFNα levels through fluorescence cell counts, with a detection sensitivity reaching 0.1×10^{-7} mg/mL. Results demonstrate that CaIFNα possesses multiple antiviral activity and activates specific ISREs, augmenting gene expression. This approach advances the study of canine ISREs and supports the development and clinical application of CaIFNα for diagnosing viral infections and monitoring treatment efficacy.

Keywords Canine interferon alpha, Fluorescent reporter assay, ISRE, Flow cytometry, Antiviral activity, EGFP

Introduction

Interferon (IFN) plays a crucial role in the immune response to viral infections, regulating and triggering innate and adaptive immune mechanisms [1]. It can inhibit the replication of various viruses [2]. Mammalian IFNs are categorized based on cell surface receptors and amino acid sequence homology into three groups, known as type I, type II, and type III IFNs [3]. Type I IFNs, primarily produced by fibroblasts and monocytes, exhibit potent antiviral activity in humans and most mammals [4]. These proteins are encoded by the IFNβ gene as well as a dozen IFNα genes and the IFN-ε, κ, τ, δ, ζ, and ω genes [5]. In response to viral challenges, IFNα/β influences myeloid cells, B cells, T cells, and NK cells, enhancing the body's immune response and promoting the generation of memory responses [6–8].

†Zhichao Pan and Yutong Liu contributed equally to this work.

*Correspondence:
Zhaoping Liang
liangzp1017@126.com
Saixiang Feng
fengsx@scau.edu.cn
[1]College of Veterinary Medicine, South China Agricultural University, Guangzhou, China
[2]Key Laboratory of Zoonosis Prevention and Control of Guangdong Province, Guangzhou, China
[3]Guangdong Laboratory for Lingnan Modern Agriculture, South China Agricultural University, Guangzhou, China
[4]Key Laboratory of Veterinary Vaccine Innovation of the Ministry of Agriculture, Guangzhou, China
[5]National and Regional Joint Engineering Laboratory for Medicament of Zoonosis Prevention and Control, Guangzhou, China

S.C. Tsai and M.J. Appel discovered canine IFN (CaIFN) while researching type I IFN in dogs [9]. Himmler et al. conducted canine species-specific studies by expressing canine IFN-α1 in *Escherichia coli* (*E. coli*) [10]. Several studies have explored the impact of different type I IFN subtypes on the immune response in dogs. Notably, the cytoplasmic localization of the canine Mx1 and Mx2 proteins was identified. Type I and III CaIFN play a crucial role in various diseases due to their effective antiviral, antitumor, and immunomodulatory properties [11]. Studies have shown that IFN-α2a inhibits angiogenesis by suppressing the production of basic fibroblast growth factor (bFGF) and vascular endothelial growth factor, thereby achieving therapeutic antitumor effects in dogs [12]. In a clinical setting, direct mucosal administration for additional oral lesions has proved to offer significant relief for dogs with epithelial lymphoma [13]. It is worth noting that while IFN-ω and IFN-α exhibit similar antiviral activity, IFN ω displays cross-species activity, unlike IFN-α [14]. Furthermore, the mucosal administration of type I IFN can serve as both a prophylactic and therapeutic agent for respiratory viral diseases in veterinary medicine.

The antiviral effects of IFNs in clinical use have been well-documented. Common methods for testing IFN activity include the cytostatic lesion assay and the luciferase reporter gene assay. The cytostatic lesion assay involves treating a cell line with dilutions of an IFN test sample and a type I IFN standard sample before infection with a viral agent such as vesicular stomatitis virus (VSV). However, this method is time consuming and dependent on viral replication. The cytopathic effect (CPE) often takes 24 h or more. Additionally, the method can only be performed in a biosafety level 3 (BSL-3) facility due to recombinant Rift Valley fever virus [15]. It is also cell-state dependent and prone to large errors between validation steps. The luciferase reporter gene method is based on type I IFN activation of the JAK-STAT signaling pathway. Type I IFNs bind to IFNAR1/IFNAR2 heterodimers, and the JAK1 and TYK2 kinases undergo phosphorylation. These phosphorylated receptors recruit and activate STAT1 and STAT2, which bind IRF9 to form a trimeric complex, IFN-stimulated gene factor (ISGF3) [16–18]. ISGF3 binds the DNA-binding protein p48 to form a transcription factor that binds a type I IFN-inducible amino acid sequence called the interferon-stimulated response elements (ISREs) and initiates transcription of ISGs [19]. Unlike the traditional antiviral assays used to evaluate type I IFNs, the luciferase reporter gene assay is an indirect method subject to various factors. Although variable results can be obtained from samples within the same batch, the effects of luciferase decay and the luminescence half-life are avoided. The study of ISREs has been extensive in humans and mice, yet relatively limited in canines [20, 21]. Currently, there is a lack of a reliable ISRE-based method for detecting the activity of canine interferon alpha (CaIFNα). However, this research, which focuses on canine ISREs, not only mitigates the impact of luciferase decay and luminescence half-life on experimental results but also fills a gap in this research area, laying a solid foundation for subsequent in-depth studies on the functions of CaIFNα and its detection methods.

In this study, we identified canine ISREs by constructing a series of reporter plasmids, detecting their biological functions through fluorescence imaging technology, and establishing a quantitative flow cytometry method based on these ISREs to detect CaIFNα activity. This work lays the groundwork for activity detection technology for both production and clinical applications.

Materials and methods

Strain, cells, and plasmids

Pichia pastoris (*P. pastoris*) GS115 was purchased from Thermo Fisher (Thermo Fisher, MA, USA). Shuffle T7 and DH5α *E. coli* were procured from New England Biolabs (NEB, MA, USA). The expression plasmids for enhanced green fluorescent protein (EGFP), VSV, and canine influenza virus (CIV) were kept in our laboratory. The H9N2 virus was provided by Professor Qi Wenbao from the College of Veterinary Medicine of South China Agricultural University. Madin–Darby canine kidney (MDCK) cells were purchased from iCell (iCell, Shanghai, China). The expression vector pET28a was preserved in our laboratory, pPICZα was purchased from Thermo Fisher, and pGL3 was purchased from Promega (Madison, Wisconsin, USA). Yeast extract peptone dextrose (YPD) medium was obtained from BD (BD, NJ, USA) and used to culture *P. pastoris* GS115 at 30 °C. Buffered-minimal Methanol Yeast extract (BMMY) and Buffered-minimal Glycerol Yeast extract (BMGY), purchased from Coolabor (Coolabor, Beijing, China) were utilized for the suspension culture of recombinant *P. pastoris* strains. MDCK cells were cultured in a 5% CO_2 incubator at 37 °C using Dulbecco's modified Eagle medium (DMEM) supplemented with 10% fetal bovine serum (FBS), both purchased from GIBCO BRL (GIBCO, NY, USA).

Expression and purification of the recombinant pET28a-CaIFNα protein with a 6 His-tag

To produce the pET28a-CaIFNα fusion protein, the amino acid sequence of CaIFNα was retrieved from NCBI (ABF68838.1). pET28a-CaIFNα was synthesized following *E. coli* preferred codon, and a 6×His tag was appended to the end of the fragment. The target gene fragment was synthesized in the pUC19 vector by Sangon Biotech (Sangon Biotech, Shanghai, China). Primers CaIFNα1-F/CaIFNα1-R were used to amplify the target gene and add *Nde*I and *Hind*III restriction sites. All

primers used are shown in Table 1. The expression vector pET28a was digested with *Hind*III and *Sac*I. Both products were recovered using a FastPure Gel DNA Extraction Mini Kit (Sangon Biotech) and ligated with T4 ligase to yield pET28a-CaIFNα. The plasmid was transformed into competent *E. coli* DH5α and incubated with 1 mM isopropyl-D-1-thiogalactopyranoside (IPTG) in Luria Bertani (LB) broth at OD_{600} = 0.2 and 16 °C for 20 h to induce expression. The cells were lysed (50 mM $NaH_2PO_4{\cdot}2H_2O$, 600 mM NaCl, 20 mM imidazole, pH 8.0) and sonicated. The lysates were centrifuged at 12,000 × g for 30 min at 4 °C, and the resulting supernatant was purified by affinity chromatography. Protein purity was assessed by SDS-PAGE, and immunoreactivity was detected by western blotting. After washing, the CaIFNα protein signal was detected with an enhanced chemiluminescence (ECL) detection system. The Micro BCA Protein Assay Kit was purchased from Thermo Fisher. Assays were performed according to the manufacturer's instructions. Protein concentrations were calculated using a linear equation based on the trend line for a standard curve generated with Microsoft Excel.

Expression and purification of recombinant CaIFNα expressed with the*P. pastoris*expression system

pPICZαA-CaIFNα was synthesized with the *P. pastoris* preferred codon, and CaIFNα was modified by adding a 6×His tag to the end of the fragment. pPICZα and the IFN gene fragment CaIFNα (cloned using primers CaIFNα2-F/CaIFNα2-R) were digested with *EcoR*I and *Xba*I and ligated with T4 ligase (primers listed in Table 1). The ligation products were transformed into competent DH5α cells by heat shock transformation. The recombinant GS115-pPICZα-CaIFNα strain was obtained after linearization of the pPICZα-CaIFNα expression plasmid by *Sac*I restriction endonuclease digestion, and the product was transferred into the receptor strain *P. pastoris* GS115, which was cultured on YPD solid medium. The recombinant strain GS115-pPICZα-CaIFNα was cultivated overnight in BMGY medium to OD_{600} ~ 1.5. The resulting cell pellets were transferred to BMMY medium supplemented with 1.5% YNB, biotin, and 0.05% methanol and incubated for 96 h. To maintain induction conditions, 0.5% sterile-filtered methanol was added every 24 h, the precipitate was discarded, and 1 mL of the culture supernatant was preserved. Purification and validation were performed as described above. The protein concentration of the purified product was determined using a Micro BCA Protein Assay Kit from Thermo Fisher, according to the manufacturer's instructions.

Assay to test suppression of the CPE in VSV and CIV infected MDCK cells

The CaIFNα protein concentration was adjusted to 0.1 mg/mL. A diluted cell suspension was prepared, and 100 μL of the cell suspension was seeded into each well of a 96-well cell culture plate, which was then incubated overnight at 37 °C and 5% CO_2. The supernatant was discarded, and protein samples in fourfold gradients were added to MDCK cells in ten columns of 100 μL per well. Culture medium was added to the last two columns as controls. The plate was incubated at 37 °C and 5% CO_2 for 18–24 h. The supernatants were discarded, and the VSV and CIV were diluted to 100 $TCID_{50}$ in infective medium. A 100 μL aliquot of the virus was added to each

Table 1 Primers used in this study

Primers	Sequence (5′ to 3′)	Description
5′AOX-F	GACTGGTTCCAATTGACAAGC	To confirm the CaIFNα integrated into the genome
3′AOX-R	GCAAATGGCATTCTGACATCC	
T7-F	TAATACGACTCACTATAGGG	To confirm the CaIFNα cloned into pET28a
T7-R	TGCTAGTTATTGCTCAGCGG	
EGFP-F	AAAGCCACCATGGTGAGCAAGGGCGAGGAG	To amplify the EGFP gene containing *Sac*I and *Hind*III restriction sites
EGFP-R	ATACAGTTCTAGATTACTTGTACAGCTCGTCCATGCC	
ISRE-F	GACGGCCAGTGAATTCGAGCTC	To amplify the interferon-stimulated response element containing *Sac*I and *Hind*III
ISRE-R	CAGCTATGACCATGATTACGCCAAGCTT	
pGL3-EGFP-F	GAGCTCGGTACCTATCGATAGAGAAATGTTCT	To amplify pGL-EGFP vector containing *Sac*I and *Hind*III
pGL3-EGFP-R	AAGCTTGGCATTCCGGTACTGTTGGTAA	
CaIFNα1-F	TCTAGCATGCATATGATGTGTCACCTCCCAG	To amplify the CaIFN gene containing *Nde*I and *Hind*III restriction sites
CaIFNα1-R	TGCAGTTTAAAGCTTTTATTTACGACGACGGAT	
P2-F	AGAAAAGAGAGGCTGAAGCTGAATTCATGTGT	To verify that the CaIFN gene has been connected to pPICZαA
P2-R	TCGACGGCGCTATTCAGATCCTCTTCTGAGATGAGTTT	
CaIFNα2-F	TCACGCCGAATTCATGTGTCACTTGCCAGACA	To amplify the CaIFN gene containing *EcoR*I and *Xba*I restriction sites
CaIFNα2-R	TCTAGATTAATGATGATGATGATGAACTTTCTTCTTCTGCGTAGA	
RVprimer4-F	CTAGCAAAATAGGCTGTCCC	To verify the construction results of plasmid pGL3-EGFP-ISRE.
RVprimer4-R	GACGATAGTCATGCCCCGCG	

well across 11 columns. The 11th column was the positive virus control group, and the 12th was the negative cellular control. The plate was incubated at 37 °C and 5% CO_2 for 24–48 h, and the results were recorded after observing a 75% CPE in the positive control by microscopy. The antiviral activity of CaIFNα was calculated using the Reed–Muench formula.

Determination of CaIFNα activity by indirect immunofluorescence assay

Before activity measurement, the protein concentration was adjusted to 0.1 mg/mL. A cell suspension was prepared by diluting cells in medium to $\sim 2 \times 10^5$ to 2.5×10^5 cells/mL. The cell suspension was added to each well of a plate. MDCK cells were treated with gradient-diluted target protein after overnight incubation. Only culture medium was added to the negative control, and positive serum was preserved in our laboratory. After 18–24 h of incubation, the H9N2 virus solution was diluted to 100 $TCID_{50}$ with serum-free DMEM and used to infect the cells. At specific time points, the cells were fixed with methanol and blocked with 1% BSA in PBST. One hour after blocking, primary mouse anti-His antibody was added (1:5000 dilution) and incubated for 1 h, followed by the addition of secondary EGFP antibody (1:5000). The results were obtained by fluorescence microscopy (Leica DM2500, Wetzlar, Germany) after washing.

Construction of ISRE reporter plasmids

The luciferase fragment was cloned from pGL3-basic-ISRE using *Nco*I and *Xba*I to obtain a vector fragment containing restriction sites. The same restriction sites were added to the EGFP gene using the specific primers (Table 1). After *Nco*I/*Xba*I digestion, the fragment and vector were ligated with T4 ligase to obtain pGL3-EGFP, which lacks the luciferase gene but contains EGFP. Bioinformatics analysis was used to predict the ISRE of CaIFNα based on the ISRE-related gene promoter region. The miniP promoter was added and submitted to Sangon Biotech for synthesis, and the pUC19-ISRE plasmid was obtained (Tables 2 and 3). The ISRE gene was amplified using ISRE-F and ISRE-R, while pGL3-EGFP-F and pGL3-EGFP-R were used to amplify the pGL3-EGFP vector with sticky ends containing *Sac*I and *Hind*III restriction sites. The ISRE and pGL3-EGFP vector fragments were ligated to yield pGL3-EGFP-ISRE (Figure S2). The primer RVprimer4-F/ RVprimer4-R was used to verify the construction results (Figure S3). Both

Table 2 Plasmids used in this study

Plasmids	Description	Source/reference
pET-28a(+)	Cloning vector, Kan^R	Millipore
pPICZαA	Cloning vector, Zeo^R	Thermo Fisher Scientific
pET-28a(+)-CaIFNα	Interferon-alpha gene cloned in pET-28a(+), Kan^R	This study
pPICZαA-CaIFNα	Interferon-alpha gene cloned in pPICZαA, Zeo^R	This study
pUC19	Cloning vector, Amp^R	This study
pUC19-ISRE1	Interferon-stimulated response element1 gene cloned in pUC19, Amp^R	This study
pUC19-ISRE2	Interferon-stimulated response element2 gene cloned in pUC19, Amp^R	This study
pUC19-ISRE3	Interferon-stimulated response element3 gene cloned in pUC19, Amp^R	This study
pUC19-ISRE4	Interferon-stimulated response element4 gene cloned in pUC19, Amp^R	This study
pUC19-ISRE5	Interferon-stimulated response element5 gene cloned in pUC19, Amp^R	This study
pUC19-ISRE6	Interferon-stimulated response element6 gene cloned in pUC19, Amp^R	This study
pUC19-ISRE7	Interferon-stimulated response element7 gene cloned in pUC19, Amp^R	This study
pUC19-ISRE8	Interferon-stimulated response element8 gene cloned in pUC19, Amp^R	This study
pUC19-ISRE9	Interferon-stimulated response element9 gene cloned in pUC19, Amp^R	This study
pUC19-ISRE10	Interferon-stimulated response element10 gene cloned in pUC19, Amp^R	This study
pGL3 basic	Expression vector, Amp^R	Promega Corporation
pEGFP-C1	Enhanced Green Fluorescent Protein gene expression vector, Kan^R	Clontech
pGL3-EGFP	Enhanced Green Fluorescent Protein gene was cloned into pGL3 basic with *Nco*I and *Xba*I, Amp^R	This study
pGL3-ISRE1-EGFP	Interferon-stimulated response element1 gene cloned in pGL3-EGFP with *Kpn*I and *Nco*I, Amp^R	This study
pGL3-ISRE2-EGFP	Interferon-stimulated response element2 gene cloned in pGL3-EGFP with *Kpn*I and *Nco*I, Amp^R	This study
pGL3-ISRE3-EGFP	Interferon-stimulated response element3 gene cloned in pGL3-EGFP with *Kpn*I and *Nco*I, Amp^R	This study
pGL3-ISRE4-EGFP	Interferon-stimulated response element4 gene cloned in pGL3-EGFP with *Kpn*I and *Nco*I, Amp^R	This study
pGL3-ISRE5-EGFP	Interferon-stimulated response element5 gene cloned in pGL3-EGFP with *Kpn*I and *Nco*I, Amp^R	This study
pGL3-ISRE6-EGFP	Interferon-stimulated response element6 gene cloned in pGL3-EGFP with *Kpn*I and *Nco*I, Amp^R	This study
pGL3-ISRE7-EGFP	Interferon-stimulated response element7 gene cloned in pGL3-EGFP with *Kpn*I and *Nco*I, Amp^R	This study
pGL3-ISRE8-EGFP	Interferon-stimulated response element8 gene cloned in pGL3-EGFP with *Kpn*I and *Nco*I, Amp^R	This study
pGL3-ISRE9-EGFP	Interferon-stimulated response element9 gene cloned in pGL3-EGFP with *Kpn*I and *Nco*I, Amp^R	This study
pGL3-ISRE10-EGFP	Interferon-stimulated response element10 gene cloned in pGL3-EGFP with *Kpn*I and *Nco*I, Amp^R	This study

Table 3 Strains used in this study

Strains	Relevant characteristic(s)	Source
E. coli DH5α	F^-, φ80d/*lacZ*ΔM15, Δ(*lacZYA-argF*) U169 *recA*1 *endA*1 *hsdR*17	New England Biolabs
BL21(DE3)	F^-, *ompT* $hsdS_B$ (r_B^-, m_B^-) *gal dcm* (DE3)	New England Biolabs
GS115	Mut^+, *his4*$^-$	Thermo Fisher Scientific
MDCK	Madin-Darby canine kidney cells, NBL-2 isolate	Laboratory stock
PZC01	BL21 carrying pET-28a (+)-CaIFNα	This study
PZC02	GS115 integrated into pPICZαA -CaIFNα	This study

pGL3-EGFP-ISRE1 and pGL3-EGFP-ISRE10 were transformed into DH5α by heat shock, and the transformants were cultured on LB agar containing 100 μg/mL ampicillin for recovery. PCR-screened single colonies and transformants were cultured in a liquid medium for storage and experiments.

Qualitative analysis of CaIFNα using an EGFP reporter plasmid

pGL3-EGFP-ISRE yield was measured by UV spectrophotometry, and the plasmid was diluted as described (Lipofectamine™ 2000). Opti-MEM® I reduced serum medium, Lipofectamine™ 2000, and pGL3-EGFP-ISRE were combined and incubated for 20 min. Cells were collected and incubated with the plasmid mixture; the medium was exchanged for medium containing serum after 4–6 h. After 24 h, the cells were stimulated with protein, and culture medium was added to the negative control group. Each group was performed in triplicate in three independent experiments. The results were obtained by fluorescence microscopy (Leica DM2500) 24 h later.

Quantitative analysis of CaIFNα activity using flow cytometry

Transfected MDCK cells were incubated as described above. After 24 h, the cells were digested with trypsin and resuspended in PBS containing 2% FBS. Next, 25 μL of 0.8% trypan blue was added to 25 μL of the cell suspension for cell counting. A total of 1×10^5 cells were recorded by flow cytometry, with the FSC set to 50, SSC set to 50, and FITC set to 8 on a BD LSRII (BD Biosciences, San Jose, CA). Data were analyzed using FlowJo version 10.6.1 (BD Biosciences). Data were analyzed using GraphPad Prism statistical software (GraphPad Software, San Diego, CA, USA). The unpaired two-tailed *t*-test was also used to analyze the data. A value of $P < 0.05$ indicated statistical significance ($^*P < 0.05$; $^{**}P < 0.01$; $^{***}P < 0.001$; and $^{****}P < 0.0001$).

Results

Expression and purification of CaIFNα in *P. pastoris*

The technical workflow used in this research is shown in Fig. 1. To compare CaIFNα expression in prokaryotic

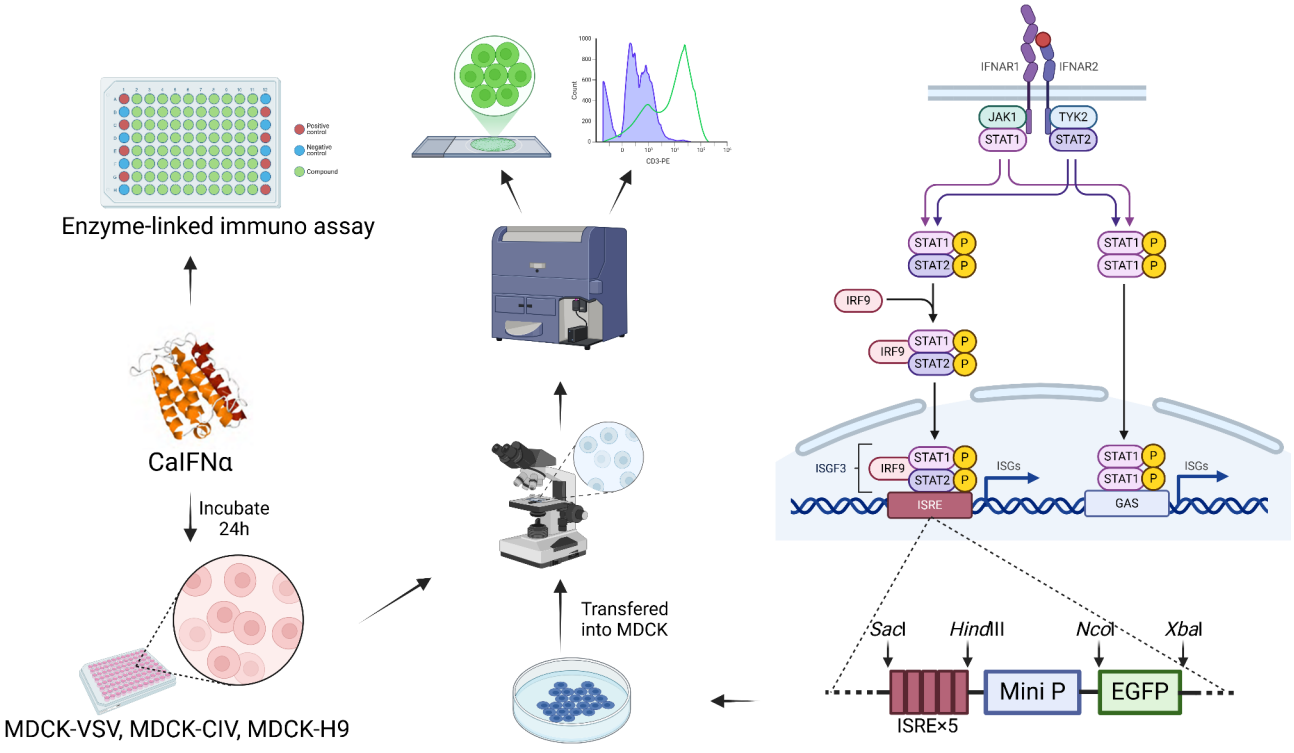

Fig. 1 Schematic illustration of CaIFNα expression by *P. pastoris* (created with BioRender)

and eukaryotic systems, we constructed a series of prokaryotic and yeast expression vectors and expressed the target protein. SDS-PAGE analysis showed that the target protein was mainly present as inclusion bodies in *E. coli* (Figure S1). The soluble protein content was low, and no distinct band was observed during SDS-PAGE analysis in the supernatant after disruption. After three independent repeated experiments, the average concentration of soluble recombinant protein expressed by the prokaryotic system was measured to be 38 μg/mL using the Micro BCA Protein Assay Kit.

The recombinant protein was expressed in a eukaryotic system with methanol added every 24 h. The culture supernatant was collected and purified for SDS-PAGE and Western blotting analysis. The data obtained showed that the target protein was successfully expressed, with clear bands visible at around 20 and 25 kDa (Fig. 2A), and the protein concentration increased slightly over time. Western blot analysis further confirmed that the band at 25 kDa corresponded to the target protein (Fig. 2B), proving that it was successfully expressed in *P. pastoris*.

After three independent repeated experiments, the concentration of the target protein expressed by the eukaryotic expression system reached 140 ± 23 μg/mL, as measured by the Micro BCA Protein Assay Kit. These findings suggest *P. pastoris* is superior to *E. coli* for expressing CaIFNα, resolving inclusion body issues.

Antiviral activity of CaIFN from *P. pastoris*

In order to assess the antiviral efficacy of CaIFNα, expressed in *P. pastoris*, against vesicular stomatitis virus (VSV) and canine influenza virus, we employed a methodology as outlined in the Materials and Methods section of this study. First, cells were treated with CaIFNα and then infected with VSV ($TCID_{50}$ = 100) for 24 h, and the CPE was observed. Cells in the control group maintained normal growth after virus infection (Fig. 3A). In contrast, cells treated with CaIFNα in the experimental group showed good antiviral effects after infection with VSV and had no significant lesions (Fig. 3B). In contrast, cells in the untreated virus control group all died under the VSV challenge (Fig. 3C). After exposing cells to four-fold CaIFNα dilutions, they were exposed to CIV for 24 h to observe cytopathic changes. No CPE was observed in the control group of cells (Fig. 3D), while cells in the virus control group died completely after CIV infection (Fig. 3F). However, the cells incubated with CaIFNα were able to resist attack from 100 $TCID_{50}$ CIV at effective concentrations (Fig. 3E). The Reed–Muench formula was used to calculate the antiviral activity. For VSV, the calculated distance ratio = (percentage of lesions above 50% – 50%) / (percentage of lesions above 50% – percentage of lesions below 50%) = (75% – 50%) / (75% – 0%) = (75% – 50%) / (75% – 0%) = 0.33. According to this formula, the antiviral activity of CaIFNα against VSV was $[4^{(9 + 0.33) \times 1}$ U / 0.1 mL] / (140 μg/mL) = 2.96×10^7 U/mg. The calculated distance ratio for CIV was (62.5% – 50%) / (62.5% – 0%) = 0.2. Therefore, the antiviral activity of CaIFNα against CIV was [4(3 + 0.2) × 1 U / 0.1 mL] / (140 μg/mL) = 6.03×10^3 U/mg. The results showed that cells incubated with CaIFNα protein expressed in *P. pastoris* remained viable after the viral attack and were effectively protected from VSV and CIV, confirming the corresponding antiviral activity of the target protein.

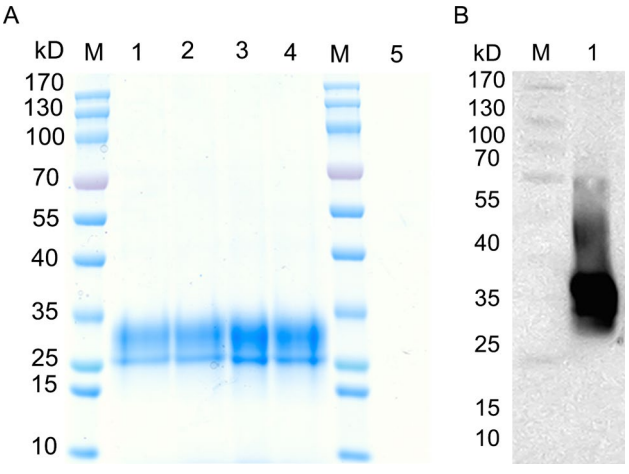

Fig. 2 Expression of the CaIFNα fusion protein. (**A**) The expression of CaIFNα grown in flasks over time was analyzed by Western blotting under reduced conditions. Lane M, Marker; lane 1, purified CaIFNα after 24 h of culture; lane 2, purified CaIFNα after 48 h of culture; lane3, purified CaIFNα after 72 h of culture; lane 4, purified CaIFNα after 96 h of culture; lane 5, GS115 96 h. (**B**) Purification of CaIFNα was analyzed by Western blot analysis. Lane M, Marker; lane 1, CaIFNα protein

CaIFNα inhibited H9 influenza virus infection in MDCK cells

To verify CaIFNα's multiple antiviral effect, we evaluated its ability to inhibit H9N2 influenza virus proliferation. Madin-Darby canine kidney (MDCK) cells were treated with various dilutions of CaIFNα and then exposed to the virus. Antiviral effect was assessed by indirect immunofluorescence assay (IFA), with fluorescence intensity serving as an indicator. The experimental results showed that the fluorescence signal of the cells in the control group was very weak, with almost no specific labeling (Fig. 4A), indicating that the control group did not receive significant antiviral protection. As the concentration of CaIFNα increased, the intensity of the fluorescence signal in the experimental group cells increased significantly, indicating that CaIFNα enhanced the protection of cells against the H9N2 virus (Fig. 4B-G). In particular, when the dilution of CaIFNα reached 4 to 9 times, although the fluorescence intensity of the experimental group was still significantly higher than that of the control group, it was slightly lower than that of the virus control group (Fig. 4H). This phenomenon shows that even at high

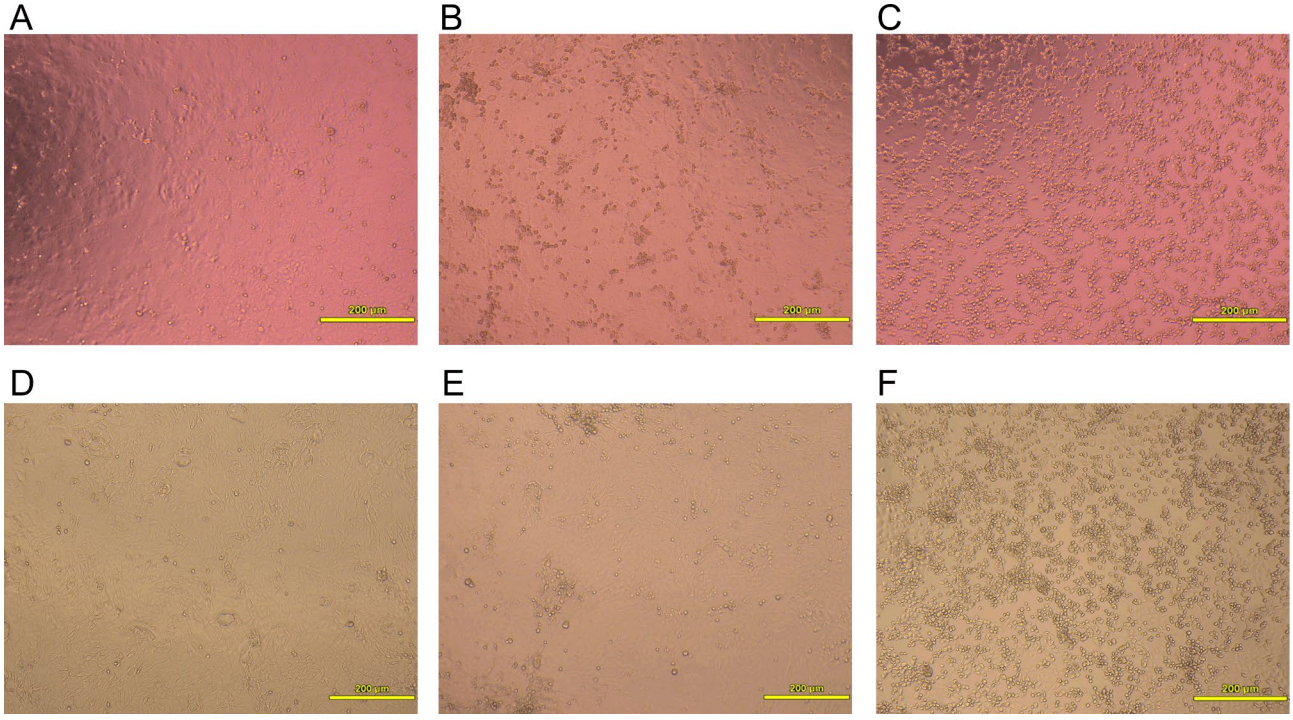

Fig. 3 Validation of the antiviral activity of CaIFNα expressed by *P. pastoris* by cytopathic inhibition assay. VSV and CIV were used to infect CaIFNα-stimulated and unstimulated MDCK cells, and changes in the cell state were observed under a microscope. All MDCK cells were inoculated with VSV or CIV at 0.1 multiplicity of infection (MOI). (**A**) MDCK cells in the control group were not infected with VSV and not treated with CaIFNα. (**B**) MDCK cells in the experimental group were infected with VSV for 24 h after incubation with CaIFNα for 24 h. (**C**) MDCK cells were infected only with VSV without the CPE of CaIFNα stimulation. (**D**) MDCK cells in the control group were not infected with CIV or treated with CaIFNα. (**E**) MDCK cells in the experimental group were incubated with CaIFNα for 24 h and then infected with CIV for 24 h. (**F**) CPE of MDCK cells infected with CIV only but not stimulated with CaIFNα

dilutions, CaIFNα can still effectively inhibit the replication of the virus and protect cells from infection.

The results demonstrate CaIFNα's multiple antiviral activity, effectively inhibiting H9N2 influenza virus replication in MDCK cells at various dilutions. This underscores its potential as an antiviral therapy, highlighting the importance of accurate measurement in its application.

Screening and identification of the canine ISRE

To establish a CaIFNα fluorescence assay, we conducted bioinformatics analysis to identify candidate ISRE sequences, screened them, and cloned the selected sequences into expression plasmids for detection (Table 4; Fig. 5). Control cells transfected with pGL3-EGFP-ISRE1, pGL3-EGFP-ISRE4, and pGL3-EGFP-ISRE6 exhibited strong background fluorescence (Fig. 5A/G/K), suggesting CaIFNα may not have caused fluorescence activation (Fig. 5B/H/L). Control cells transfected with pGL3-EGFP-ISRE3, pGL3-EGFP-ISRE5, pGL3-EGFP-ISRE7, and pGL3-EGFP-ISRE9 showed weak non-specific fluorescence (Fig. 5E/I/M/Q), and the experimental group exhibited no significant fluorescence after stimulation with CaIFNα (Fig. 5F/J/N/R). Thus, ISRE3, ISRE5, ISRE7, and ISRE9 may not be valid canine ISREs. In contrast, the experimental groups transfected with pGL3-EGFP-ISRE2, pGL3-EGFP-ISRE8, and pGL3-EGFP-ISRE10 produced strong fluorescence (Fig. 5C–D/O–P/S–T) upon stimulation with CaIFNα, significantly different from the transfected controls. Thus, CaIFNα activates ISRE2, ISRE8, and ISRE10 to promote expression of EGFP in the plasmid constructs, indicating that they are effective ISREs that serve as pivotal components for precisely evaluating the activity of CaIFNα.

ISRE-based quantitative analysis of CaIFNα activity by flow cytometry

Flow cytometry was used to quantify the activation of ISRE sequences by CaIFNα. Given the IFA results, we selected ISRE2, ISRE8, and ISRE10 for detection. Flow histograms demonstrated that ISRE-transfected MDCK cells fluoresced more after CaIFNα stimulation. In the experimental group of ISRE2 transfectants, P2 showed a 20.78% increase in the average number of fluorescent cells after stimulation compared to the control group (Fig. 6A–B). Whereas, the number of fluorescent ISRE8-transfected cells was increased by 21.44% (Fig. 6C–D) and 16.73% in the ISRE10-transfected cells (Fig. 6E–F).

Flow cytometry results identified ISRE8 as the best sequence, which was selected for quantitative

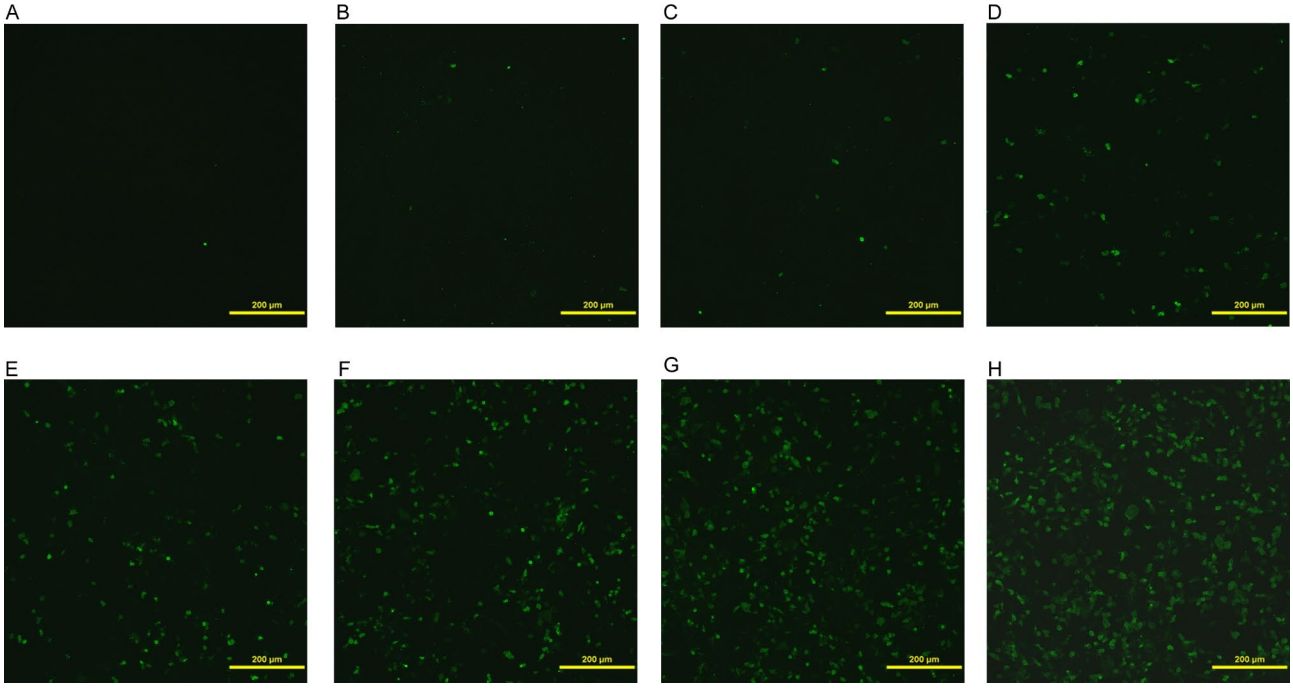

Fig. 4 Identification of the inhibitory effect of CaIFNα against H9N2 subtype influenza virus by IFA. After diluting CaIFNα from the concentration of 0.1×4^{-4} mg/mL to 0.1×4^{-9} mg/mL, MDCK cells were incubated with CaIFNα. After 24 h of incubation, the cells were infected with H9N2 for 24 h. Fluorescence signals were observed to detect the presence of the H9N2 virus hemagglutinin (HA). A: MDCK cells in the control group were neither stimulated with CaIFNα nor infected with H9. B-G: MDCK cells were infected with H9N2 after stimulation with CaIFNα serially diluted from 0.1×4^{-4} mg/mL to 0.1×4^{-9} mg/mL. H: MDCK cells without CaIFNα treatment were infected with H9N2

Table 4 The predicted sequences of the ISREs for CaIFNα

Name	Promoter Sequence of ISRE (5′-3′)	Size(bp)
ISRE1	TAGTTT**CG**TTTCCC	14
ISRE2	TAGTTT**CA**TTTCCC	14
ISRE3	TAGTTT**CC**TTTCCC	14
ISRE4	TAGTTT**CAC**TTTCCC	15
ISRE5	TAGTTT**CAG**TTTCCC	15
ISRE6	TAGTTT**GA**TTTCCC	14
ISRE7	TACTTT**CC**TTTCCC	14
ISRE8	TAGTTT**TGT**TTTCCC	15
ISRE9	TAGTTT**TG**TTTCCC	14
ISRE10	TAGTTT**CCT**TTTCCC	15

verification. After transfection with ISRE8, cells were desensitized with a CaIFNα dilution series and analyzed by flow cytometry. The results showed a decrease in fluorescent cells with increasing IFN dilution (Fig. 7). After four repeated experiments, the average proportion of fluorescent cells in the control group was 2.66% ± 0.42% and at IFN 4^{-1}, the average proportion of fluorescent cells increased to 19.91% ± 1.82% ($P<0.001$). At dilutions of 4^{-2}, 4^{-3}, 4^{-4}, and 4^{-5}, the proportions fluorescent cells dropped to 19.34% ± 3.38%, 17.01% ± 2.51%, 17.62% ± 2.30%, and 13.17% ± 2.02% ($P<0.01$). At 4^{-6} and 4^{-7}, fluorescence dropped to 9.77% ± 2.27% and 6.32% ± 1.15%, respectively ($P<0.05$). At 4^{-8}, fluorescence was 4.45% ± 0.71%. Analysis by *t*-test showed that the activation activity in the stimulated group significantly differed from that of the control group, even at CaIFNα 4^{-7} ($P<0.05$). The results showed that the plasmid was successfully transfected into MDCK cells. Upon stimulation with CaIFNα, the CaIFNα ISRE sequence was activated, and the expression of downstream EGFP was activated. At even low concentrations, CaIFNα retained its activation activity, validating the high sensitivity of the method, which underscores the significance of identifying effective ISREs in accurately assessing CaIFNα activity, thereby advancing our understanding of CaIFNα as an antiviral substance and laying the foundation for its further study.

Discussion

ISREs are DNA sequences crucial for cellular immune responses, regulating interferon-responsive genes, exerting antiviral effects, and stimulating inflammation [22, 23]. IFNα and IFNγ regulate interferon-stimulated genes (ISG) expression by recruiting transcription factors such as ISGF3 and GAF, to the ISRE and gamma IFN activation sequence (GAS) complex sites [24]. The ISRE + GAS site acts as a molecular switch that regulates gene expression based on the available components and timing of transcription factor complex formation [25]. This fine-tuned regulation is particularly crucial for many ISGs, which exhibit remarkable versatility by demonstrating

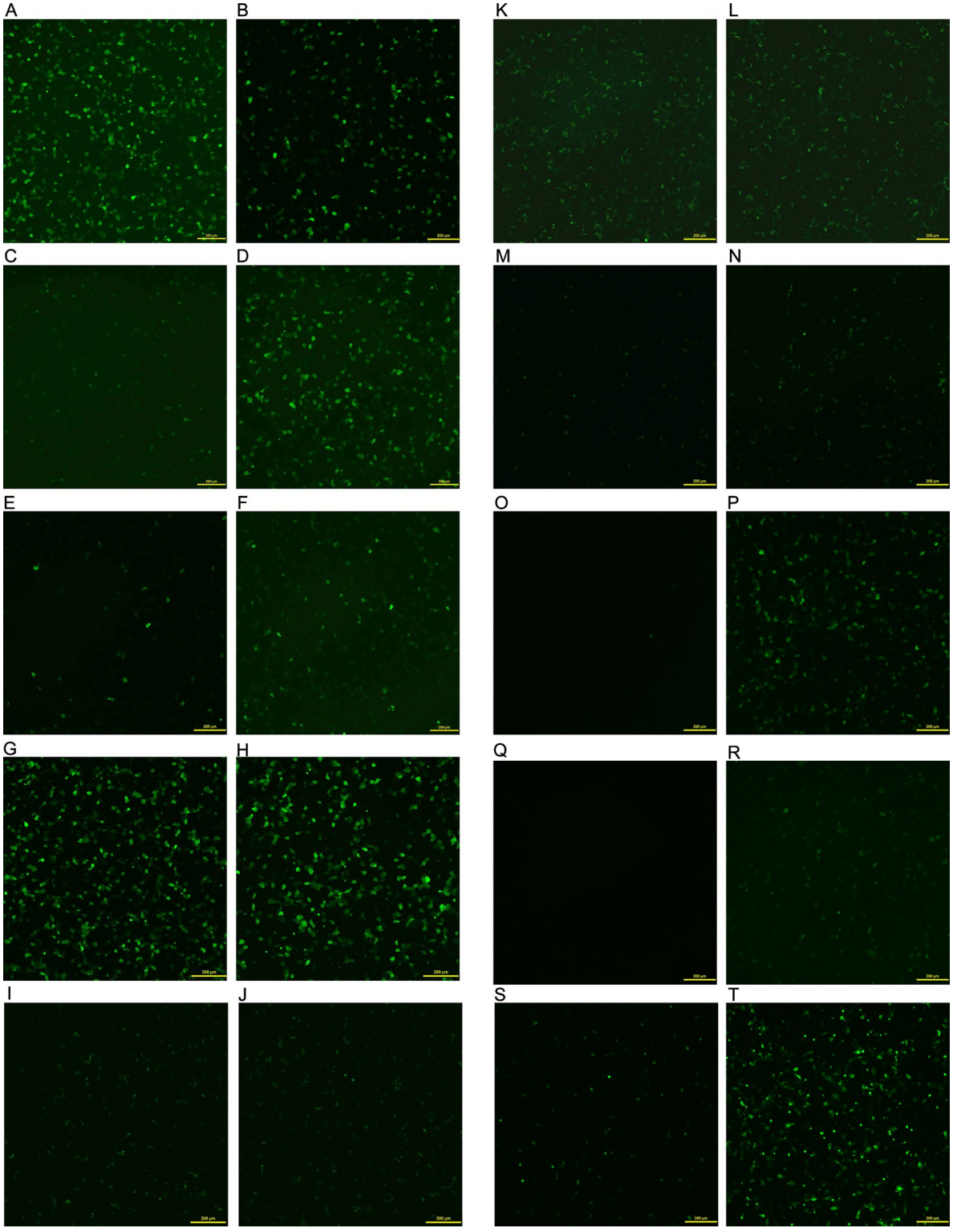

Fig. 5 Screening of canine ISRE sequences sensitive to CaIFNα using fluorescence detection. A/C/E/G/I/K/M/O/Q/S: MDCK cells were transfected with plasmid pGL3-EGFP containing different ISRE sequences (ISRE1 to ISRE10). The cells were then stimulated with CaIFNα. The expression of green fluorescent protein (EGFP) was observed under a fluorescence microscope to evaluate the sensitivity of each ISRE sequence to CaIFNα. B/D/F/H/J/L/N/P/R/T: MDCK cells were transfected with the same plasmids as above, but this time without CaIFNα stimulation, serving as controls. The fluorescence images illustrate the differences in EGFP expression levels between cells treated and not treated with CaIFNα

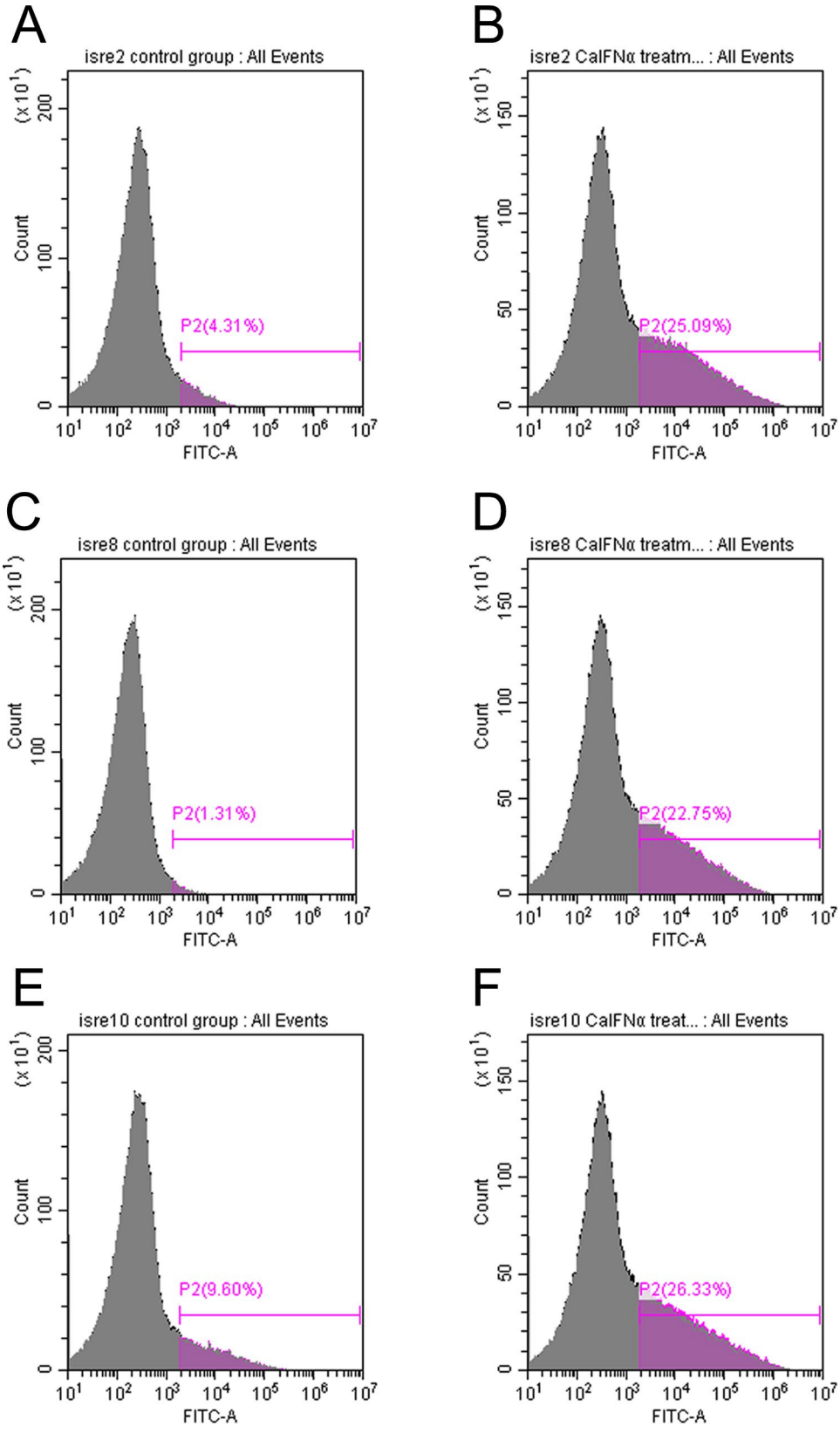

Fig. 6 (See legend on next page.)

(See figure on previous page.)

Fig. 6 The response of ISRE2/ISRE8/ISRE10 to CaIFNα was further quantified by flow cytometry. After the corresponding plasmids containing ISRE2/ISRE8/ISRE10 were transfected into MDCK cells, the cells were stimulated by CaIFNα, and the proportion of cells emitting fluorescence was calculated by flow cytometry. A/C/E: Control MDCK cells were transfected with the ISRE2/ISRE8/ISRE10 plasmids without CaIFNα stimulation. B/D/H: The fluorescence levels of MDCK cells transfected with ISRE2/ISRE8/ISRE10 and stimulated with the CaIFNα protein were measured. P values reflect the proportion of cells that were fluorescent

broad-spectrum antiviral activity against a wide range of viral families [19]. Intriguingly, studies have revealed that the base composition and arrangement of ISRE sequences vary significantly between species, suggesting a layer of complexity in the regulation of ISG expression [26, 27]. These differences may result in various species responding differently to INF signaling and gene expression. For instance, ISRE sequences in humans and fish have different base compositions at certain sites, affecting thereby influencing binding of response elements and the activation of response factors [28]. Thus, the species specificity of ISREs may lead to differences in the immune response. ISRE activation promotes the transcription of ISGs, which induce expression of various antiviral proteins [29]. Species-specific ISRE sequences in humans, rodents, fish, and birds have been identified, but canine-specific ISREs have not been previously identified. Further study of ISRE species specificity could provide insight into species-level immune system differences and provide more precise and effective strategies for treating pets. These findings suggest that ISREs play a critical role in the antiviral effects of INFs.

Most IFN activity assays are based on cytopathic inhibition and 3-(4,5-dimethylthiazol-2-yl)-2,5-diphenyltetrazolium bromide (MTT) methods, but these have limitations. The cytopathic inhibition method is highly dependent on culture density and status, and experimental reproducibility is relatively poor [30]. The MTT method requires that the methanogenic products produced after reduction be dissolved before detection. The method also requires lysis before detection and is influenced by many factors, such as changes in cellular metabolism and oxidoreductase activity [31], significantly impacting readouts. The optimal reaction time is 30 min; obvious errors will occur beyond this point. One previous study improved the MTT method for bacteria and established an equation that relates colony-forming units to the amount of formazan converted by bacteria [32]. Moghawry proposed using flow cytometry to replace colony-forming unit (CFU) and MTT assays for Bacillus Calmette–Guérin vaccine quality control, as it can distinguish abnormal cells, automate testing, and improve efficiency and accuracy [33]. Numerous factors influence the luciferase reporter gene assay, and the data from the same batch of samples may fluctuate. The binding, active, and catalytic sites are crucial for luciferase activity [33]. At the same time, the use of this technology is limited by the high cost of substrates such as d-luciferin. In 2023, a study proposed using membrane-bound horseradish peroxidase (mHRP) as a new reporter system [34]. This system uses less expensive HRP substrates, avoids the cell lysis process and expensive luciferase substrates, and is suitable for high-throughput analysis. Furthermore, avoiding the effects of luciferase decay and the luminescence half-life is important. Other studies have designed a standard curve program based on MxA gene expression and interferon antiviral activity (IU/ml) relative to qPCR data processing to evaluate the antiviral effects of interferons α, β, and γ [35]. However, this method requires high sample purity, and any contamination during sample processing may lead to false positive results, especially when other viruses or interfering substances are mixed into the sample. In addition, qPCR technology itself has limitations such as reaction condition optimization, instrument accuracy and stability, which may affect the accuracy and reliability of the test results. Antiviral assays are the most widely used methods to detect IFN activity, but no international standard has been proposed for research on IFNα by WHO [36]. Laboratories that can cultivate viruses may choose an antiviral assay; however, most laboratories do not have this capability and prefer to use non-virological methods. In these cases, the specificity of the measured IFN antiviral activity and assay reproducibility must be carefully considered. In this study, we generated ISG for the CaIFNα-induced ISRE sequence, constructed the reporter plasmid pGL3-EGFP-ISRE by replacing the luciferase reporter gene with EGFP, and used flow cytometry to measure EGFP fluorescence as an indicator of CaIFNα activity. This method improves upon previous ones by offering advantages like no need for cell permeability or exogenous substrates, enhanced biosafety, sensitivity, and time efficiency. It also reduces the risk of harmful virus transmission and infection in type I IFN bioassays. However, this method still exhibits certain limitations. Flow cytometry, as a highly specialized technique, necessitates costly equipment and professional operational skills, thereby limiting its widespread application in laboratories with limited resources or inadequate technical conditions. Although the ISRE and EGFP-based method offers intuitive fluorescent signals to indicate IFN activity, the settings of flow cytometers, parameter adjustments, and data analysis methods may vary among different laboratories, leading to difficulties in standardizing the data and compromising the comparability of data among laboratories. Furthermore, differences in cell types may also affect the accuracy and

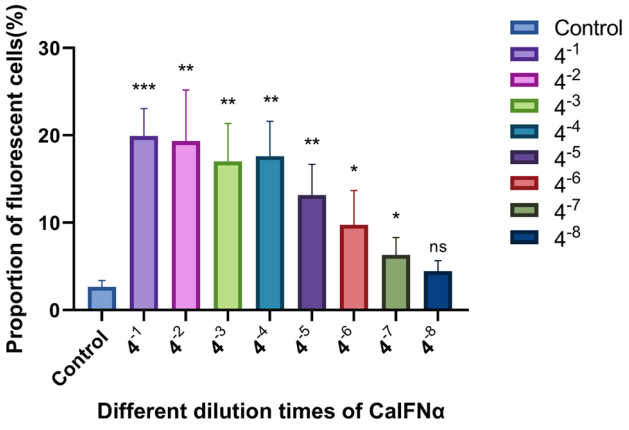

Fig. 7 Verification that fluorescence intensity varied with CaIFNα concentration by flow cytometry. MDCK cells transfected with the ISRE8 reporter plasmid pGL3-EGFP-ISRE8 were treated with gradient dilutions of CaIFNα (dilution factor 4^{-1} to 4^{-8}). After treatment, the cells could directly produce strong fluorescence, so flow cytometry was used Measure fluorescence intensity. Lane 1: Unstimulated control group. Lanes 2–9: Serial dilutions of CaIFNα-treated MDCK cells. The proportion of fluorescent cells reflects CaIFNα activity. Fluorescence intensity was measured using BD LSRII, and data represent mean ± SEM. Statistical significance was determined by unpaired *t*-test; ns means no significance, **P* < 0.05, ***P* < 0.01, ****P* < 0.001, *****P* < 0.0001

sensitivity of the method. In this experiment, MDCK cells were used, which exhibit minimal interference from endogenous fluorescent backgrounds; however, if metabolically active cells are employed, the abundant NADPH produced within them may interfere with the accurate measurement of EGFP signals.

Utilizing a yeast (eukaryotic) expression system allows the proper folding and posttranslational modification of the expressed protein. Glycosylation, a common modification, is categorized as N-glycosylation and O-glycosylation based on sugar-amino acid linkages. N-Glycosylation typically happens at asparagine residues in the sequence Asn-X-Ser/Thr, where X cannot be proline due to its structural inhibition [37, 38]. The central enzyme in the N-glycosylation pathway is oligosaccharyltransferase, which catalyzes the formation of N-glycosidic bonds between oligosaccharides and the side chain amide of asparagine. In yeast, O-linked glycosylation occurs by binding serine or threonine to mannose residues [39]. In this study, CaIFNα had a slightly higher molecular weight than the predicted 25 kDa, suggesting glycosylation by yeast. Western blot analysis showed that the smallest band corresponded to a molecular weight of approximately 20 kDa, and the largest band corresponded to approximately 25 kDa. The band may correspond to a molecular weight smaller than 25 kDa because glycosylation was not complete or absent. Wang et al. removed glycosylation sites from bovine enterokinase using site-directed mutagenesis and found that the recombinant protein's molecular weight decreased after deglycosylation, resulting in a more uniform band [40]. Furthermore, they found that the N-glycosylation of urokinase did not significantly affect its expression in *P. pastoris*. Similarly, Han et al. demonstrated that introducing N-glycosylation sites into recombinant elastase enhanced the synthesis rate and yield of the target protein [41]. Another study introduced a free radical activation strategy to obtain multifunctional and stereoselective N-glycosylation to show excellent tolerability [42]. This study compared CaIFNα expression by *E. coli* and *P. pastoris*. Even though glycosylated IFN existed in the yeast system, the modified protein still had biological activity. Although this study successfully developed an ISRE and EGFP-based flow cytometry method to measure the biological activity of CaIFNα, several aspects can be further expanded and improved. First, in addition to the VSV, CIV, and H9N2 viruses tested in this study, future evaluations of other common canine viruses, such as canine distemper virus and canine parvovirus, should be considered to understand the antiviral potential of CaIFNα fully. In addition, although the current method has a high sensitivity, technologies that further improve the detection accuracy, such as optimizing the flow cytometer settings or introducing more efficient fluorescent labels, may be helpful.

Conclusion

In this study, we achieved secretory expression of CaIFNα in *P. pastoris*. The purified protein demonstrated antiviral activity against VSV, CIV, and H9 influenza virus, verifying its functionality. Additionally, canine ISRE components were identified, and a new method for detecting CaIFNα's biological activity via ISRE-based flow cytometry was developed. This approach lays a foundation for the activity quantification and further research of CaIFNα.

Abbreviations

bFGF	Basic fibroblast growth factor
BMGY	Buffered-minimal Glycerol Yeast extract
BMMY	Buffered-minimal Methanol Yeast extract
BSL-3	Biosafety level 3
Canine	IFN α CaIFNα
CIV	Canine influenza virus
CFU	Colony-forming unit
CPE	Cytopathic effect
DMEM	Dulbecco's modified Eagle medium
E. coli	Escherichia coli
ECL	Enhanced chemiluminescence
EGFP	Enhanced green fluorescent protein
IFA	Indirect immunofluorescence assay
IFN	Interferon
IPTG	Isopropyl-D-1-thiogalactopyranoside
ISGF3	IFN-stimulated gene factor
ISRE	Interferon-stimulated response elements
LB	Luria Bertani
MDCK	Madin-Darby canine kidney
MTT	3-(4,5-dimethylthiazol-2-yl)-2,5-diphenyltetrazolium bromide
P. pastoris	Pichia pastoris
VSV	Vesicular stomatitis virus

YPD Yeast extract peptone dextrose

Supplementary Information

The online version contains supplementary material available at https://doi.org/10.1186/s12917-025-04577-3.

Supplementary Material 1

Acknowledgements
The authors express gratitude to Dr. Qi Wenbao from the College of Veterinary Medicine of South China Agricultural University for providing H9N2 virus.

Author contributions
The study was conceptualised and designed by SF. ZP carried out the methodology, and investigation. YL, HD and SX performed formal analysis and verification. MQ, KW and CL provided resources. CL and QZ visualized the experimental results. The first manuscript draft was written by ZP and YL. ZL performed experimental supervision. All authors commented on early versions of the manuscript, read, modified and approved the final version. Figure 1 created with BioRender released under a Creative Commons Attribution-NonCommercial-NoDerivs 4.0 International license.

Funding
This work was supported by the National Key Research and Development Program of China (2022YFD1801003).

Data availability
No datasets were generated or analysed during the current study.

Declarations

Ethics approval and consent to participate
Not applicable.

Consent for publication
Not applicable.

Competing interests
The authors declare no competing interests.

Received: 15 October 2024 / Accepted: 7 February 2025
Published online: 01 March 2025

References

1. Malmgaard L. Induction and regulation of IFNs during viral infections. J Interferon Cytokine Res. 2004;24(8):439–54.
2. Taylor MW. Interferons. In: Viruses and Man: A History of Interactions. edn.; 2014: 101–119.
3. Fensterl V, Sen GC. Interferons and viral infections. BioFactors. 2009;35(1):14–20.
4. Parkin J, Cohen B. An overview of the immune system. Lancet. 2001;357(9270):1777–89.
5. Levy DE, Marié IJ, Durbin JE. Induction and function of type I and III interferon in response to viral infection. Curr Opin Virol. 2011;1(6):476–86.
6. McNab F, Mayer-Barber K, Sher A, Wack A, O'Garra A. Type I interferons in infectious disease. Nat Rev Immunol. 2015;15(2):87–103.
7. Harper J, Huot N, Micci L, Tharp G, King C, Rascle P, Shenvi N, Wang H, Galardi C, Upadhyay AA, et al. IL-21 and IFNα therapy rescues terminally differentiated NK cells and limits SIV reservoir in ART-treated macaques. Nat Commun. 2021;12(1):2866.
8. Shemesh M, Aktepe TE, Deerain JM, McAuley JL, Audsley MD, David CT, Purcell DFJ, Urin V, Hartmann R, Moseley GW, et al. Correction: SARS-CoV-2 suppresses IFNβ production mediated by NSP1, 5, 6, 15, ORF6 and ORF7b but does not suppress the effects of added interferon. PLoS Pathog. 2021;17(12):e1010146.
9. Tsai SC, Appel MJ. Interferon induction in dogs. Am J Vet Res. 1979;40(3):356–61.
10. Himmler A, Hauptmann R, Adolf GR, Swetly P. Structure and expression in *Escherichia coli* of canine interferon-alpha genes. J Interferon Res. 1987;7(2):173–83.
11. Nakamura T, Asano A, Okano S, Ko JH, Kon Y, Watanabe T, Agui T. Intracellular localization and antiviral property of canine Mx proteins. J Interferon Cytokine Res. 2005;25(3):169–73.
12. Clifford CA, Mackin AJ, Henry CJ. Treatment of canine hemangiosarcoma: 2000 and beyond. J Vet Intern Med. 2000;14(5):479–85.
13. Tzannes S, Ibarrola P, Batchelor DJ, Burrow RD, Blackwood L. Use of recombinant human interferon alpha-2a in the management of a dog with epitheliotropic lymphoma. J Am Anim Hosp Assoc. 2008;44(5):276–82.
14. Luo X, Guo Y, Bao J, Liu Y, An D, Ma B, Gao M, Wang J. Characterization and antivirus activities of a novel bovine IFN-omega24. Mol Immunol. 2015;66(2):357–63.
15. Kuri T, Habjan M, Penski N, Weber F. Species-independent bioassay for sensitive quantification of antiviral type I interferons. Virol J. 2010;7:50.
16. Zitvogel L, Galluzzi L, Kepp O, Smyth MJ, Kroemer G. Type I interferons in anticancer immunity. Nat Rev Immunol. 2015;15(7):405–14.
17. Cho H, Kelsall BL. The role of type I interferons in intestinal infection, homeostasis, and inflammation. Immunol Rev. 2014;260(1):145–67.
18. Lazear HM, Schoggins JW, Diamond MS. Shared and distinct functions of type I and type III interferons. Immunity. 2019;50(4):907–23.
19. Swaraj S, Tripathi S. Interference without interferon: interferon-independent induction of interferon-stimulated genes and its role in cellular innate immunity. mBio. 2024;15(10):e02582–02524.
20. Uccellini MB, García-Sastre A. ISRE-Reporter mouse reveals high basal and Induced Type I IFN responses in inflammatory monocytes. Cell Rep. 2018;25(10):2784–e27962783.
21. Taura M, Frank JA, Takahashi T, Kong Y, Kudo E, Song E, Tokuyama M, Iwasaki A. APOBEC3A regulates transcription from interferon-stimulated response elements. Proceedings of the National Academy of Sciences 2022, 119(20):e2011665119.
22. Leviyang S. Interferon stimulated binding of ISRE is cell type specific and is predicted by homeostatic chromatin state. Cytokine X. 2021;3(4):100056.
23. Cui D, Espínola Emilio E, Arora K, Brinton Margo A. Two Interferon-stimulated response elements cooperatively regulate Interferon-stimulated gene expression in West Nile Virus-infected IFNAR–/– mouse embryo fibroblasts. J Virol. 2021;95(22). https://doi.org/10.1128/jvi.01040–01021.
24. Da G, Wang J, Shang J, Xun C, Yu Y, Wang Y, Tie N, Li H. Nuclear PCGF3 inhibits the antiviral immune response by suppressing the interferon-stimulated gene. Cell Death Discovery. 2024;10(1):429.
25. Sekrecka A, Kluzek K, Sekrecki M, Boroujeni ME, Hassani S, Yamauchi S, Sada K, Wesoly J, Bluyssen HAR. Time-dependent recruitment of GAF, ISGF3 and IRF1 complexes shapes IFNα and IFNγ-activated transcriptional responses and explains mechanistic and functional overlap. Cell Mol Life Sci. 2023;80(7):187.
26. Sheikh SZ, Kobayashi T, Matsuoka K, Onyiah JC, Plevy SE. Characterization of an interferon-stimulated response element (ISRE) in the Il23a promoter. J Biol Chem. 2011;286(2):1174–80.
27. Gongora C, Degols G, Espert L, Hua TD, Mechti N. A unique ISRE, in the TATA-less human Isg20 promoter, confers IRF-1-mediated responsiveness to both interferon type I and type II. Nucleic Acids Res. 2000;28(12):2333–41.
28. Levraud JP, Jouneau L, Briolat V, Laghi V, Boudinot P. IFN-Stimulated genes in zebrafish and humans define an ancient arsenal of antiviral immunity. J Immunol. 2019;203(12):3361–73.
29. Zhou JH, Wang YN, Chang QY, Ma P, Hu Y, Cao X. Type III interferons in viral infection and antiviral immunity. Cell Physiol Biochem. 2018;51(1):173–85.
30. Iwata A, Iwata NM, Saito T, Hamada K, Sokawa Y, Ueda S. Cytopathic effect inhibition assay for canine interferon activity. J Vet Med Sci. 1996;58(1):23–7.
31. Hawser S. Adhesion of different Candida spp. to plastic: XTT formazan determinations. J Med Vet Mycol. 1996;34(6):407–10.
32. Xu W, Shi D, Chen K, Palmer J, Popovich DG. An improved MTT colorimetric method for rapid viable bacteria counting. J Microbiol Methods. 2023;214:106830.
33. Moghawry HM, Rashed ME, Gomaa K, AbdelGhani S, Dishisha T. Development of a fast and precise potency test for BCG vaccine viability using flow cytometry compared to MTT and colony-forming unit assays. Sci Rep. 2023;13(1):11606.
34. Chang MS, Lee CY, Liu ES, Chao H, Wu HY, Chang YY, Liu YL, Chen YT, Su YC, Wang YT, et al. A Low-Cost, sensitive reporter system using

membrane-tethered horseradish peroxidase for efficient gene expression analysis. Anal Chem. 2023;95(38):14341–9.
35. Saber MA, Okasha H, Khorshed F, Samir S. A novel cell-based in vitro assay for antiviral activity of interferons α, β, and γ by qPCR of MxA Gene expression. Recent Patents Biotechnol. 2021;15(1):67–75.
36. Meager A, Gaines Das R, Zoon K, Mire-Sluis A. Establishment of new and replacement World Health Organization International Biological Standards for human interferon alpha and omega. J Immunol Methods. 2001;257(1–2):17–33.
37. Schjoldager KT, Narimatsu Y, Joshi HJ, Clausen H. Global view of human protein glycosylation pathways and functions. Nat Rev Mol Cell Biol. 2020;21(12):729–49.
38. Esmail S, Manolson MF. Advances in understanding N-glycosylation structure, function, and regulation in health and disease. Eur J Cell Biol. 2021;100(7–8):151186.
39. Bretthauer RK, Castellino FJ. Glycosylation of *Pichia pastoris*-derived proteins. Biotechnol Appl Biochem. 1999;30(3):193–200.
40. Wang Z, Guo C, Liu L, Huang H. Effects of N-glycosylation on the biochemical properties of recombinant bEK(L) expressed in *Pichia pastoris*. Enzyme Microb Technol. 2018;114:40–7.
41. Han M, Wang X, Yan G, Wang W, Tao Y, Liu X, Cao H, Yu X. Modification of recombinant elastase expressed in *Pichia pastoris* by introduction of N-glycosylation sites. J Biotechnol. 2014;171:3–7.
42. Ding W, Chen X, Sun Z, Luo J, Wang S, Lu Q, Ma J, Zhao C, Chen FE, Xu C. A Radical Activation Strategy for Versatile and Stereoselective N-Glycosylation. Angewandte Chemie (International ed in English) 2024, 63(36):e202409004.

Publisher's note